

Basilar Membrane Responses to Noise at a Basal Site of the Chinchilla Cochlea: Quasi-Linear Filtering

ALBERTO RECIO-SPINOSO¹, SHYAMLA S. NARAYAN², AND MARIO A. RUGGERO³

¹ENT Department, Leiden University Medical Center, Postbus 9600 2300 RC, Leiden, The Netherlands

²2748 Palm Springs Lane, Aurora, IL 60502, USA

³Department of Communication Sciences and Disorders, Northwestern University, 2240 Campus Drive, Evanston, IL 60208, USA

Received: 15 January 2009; Accepted: 28 April 2009; Online publication: 3 June 2009

ABSTRACT

Basilar membrane responses to clicks and to white noise were recorded using laser velocimetry at basal sites of the chinchilla cochlea with characteristic frequencies near 10 kHz. Responses to noise grew at compressive rates and their instantaneous frequencies decreased with increasing stimulus level. First-order Wiener kernels were computed by cross-correlation of the noise stimuli and the responses. For linear systems, first-order Wiener kernels are identical to unit impulse responses. In the case of basilar membrane responses, first-order Wiener kernels and responses to clicks measured at the same sites were similar but not identical. Both consisted of transient oscillations with onset frequencies which increased rapidly, over about 0.5 ms, from 4–5 kHz to the characteristic frequency. Both first-order Wiener kernels and responses to clicks were more highly damped, exhibited slower frequency modulation, and grew at compressive rates with increasing stimulus levels. Responses to clicks had longer durations than the Wiener kernels. The statistical distribution of basilar membrane responses to Gaussian white noise is also Gaussian and the envelopes of the responses are Rayleigh distributed, as they should be for Gaussian noise passing through a linear band-pass filter. Accordingly, basilar membrane responses were accurately predicted by linear filters specified by the first-order Wiener kernels of responses to noise

presented at the same level. Overall, the results indicate that cochlear nonlinearity is not instantaneous and resembles automatic gain control.

Keywords: Wiener kernels, clicks, laser velocimetry, frequency glides, impulse responses

INTRODUCTION

Basilar membrane (BM) vibrations exhibit a peculiar type of nonlinearity characterized by responses to tones with low waveform distortion (Cooper 1998; Rhode 2007; Ruggero et al. 1997) but magnitudes that grow at highly compressive rates with increasing stimulus level (Robles and Ruggero 2001). In this study, we evaluate the linear and nonlinear features of BM vibrations using Gaussian white noise stimuli and Wiener kernel analysis. For many types of nonlinear systems, it is possible to relate inputs and outputs using sums of functionals (i.e., functions of functions) derived from responses to white noise. Such functional series, originally derived by Volterra (1959), were first applied by Norbert Wiener to the study of nonlinear systems (Marmarelis and Marmarelis 1978). His method, “Wiener kernel analysis,” is a nonparametric approach to system modeling and does not require *a priori* knowledge of the internal structure of the system. For linear systems, the first-order Wiener kernel is identical to the unit impulse response and hence permits the prediction of system responses to arbitrary stimuli. For nonlinear systems, the first-order kernel provides a linear approximation to the system, containing the linear component plus possible contributions from odd-order

Correspondence to: Mario A. Ruggero · Department of Communication Sciences and Disorders · Northwestern University · 2240 Campus Drive, Evanston, IL 60208, USA. Telephone: +1-847-4913180; fax: +1-847-5912523; email: mruggero@northwestern.edu

nonlinearities. Second-order kernels contain second-order plus possible higher even-order nonlinearities (Marmarelis and Marmarelis 1978).

Wiener kernels have been used to analyze responses to noise of auditory nerve fibers (e.g., Carney and Yin 1988; de Boer 1967; Evans 1977; Møller 1977; Recio-Spinoso et al. 2005), cochlear nucleus neurons (Wickesberg et al. 1984), and basal BM sites of the guinea pig cochlea (de Boer and Nuttall 1997, 2000). At the guinea pig BM, first-order Wiener kernels resemble responses to clicks in several respects, including the presence of an initial increase in the frequency of oscillation (the “glide”) thought to be invariant across stimulus levels. In this paper, we describe responses to clicks and the first-order Wiener kernels of BM responses to white noise stimuli measured at the same basal sites of chinchilla cochleae. Our main findings are that: (1) the frequency modulation at the onset of Wiener kernels varies as a function of stimulus level; (2) first-order Wiener kernels of responses to noise closely resemble, but are more damped than, responses to clicks; and (3) in spite of cochlear nonlinearities, linear filtering using Wiener kernels accurately predicts BM responses to white noise presented at the same levels. A preliminary report of this investigation was published in the proceedings of a conference (Recio et al. 1997).

METHODS

Animal preparation and data collection

Animal preparations were similar to those described in previous BM studies in our laboratory (Recio et al. 1998; Ruggero et al. 1997). Briefly, adult chinchillas (average weight=500 g) were anesthetized with an initial injection of ketamine (100 mg/kg, s.c.) followed by sodium pentobarbital (65 mg/kg, i.p.). The initial dose of pentobarbital was supplemented by smaller additional doses to maintain a complete absence of limb withdrawal reflexes. Rectal temperature of the animals was maintained at 38°C with a servo-controlled electrical heating pad. Tracheotomy and tracheal intubation allowed for forced respiration, which was used only as necessitated by apnea or labored breathing. The pinna was resected and part of the bony external ear canal was chipped away to permit visualization of the umbo of the tympanic membrane and insertion of the earphone coupling speculum. After opening the bulla widely, the tendon of the tensor tympani muscle was severed and the stapedius muscle was detached from its bony anchoring to prevent possible effects of muscle contraction evoked by high-level acoustic stimuli. A silver ball electrode was placed on the round window to monitor cochlear health by measuring compound action potential thresholds.

A small hole was made in the basal turn of the otic capsule by first thinning and drilling the bone using a dental bur and then chipping away bone fragments with a metal pick. The hole allowed direct visualization of the BM at a site located approximately 3.5 mm from the oval window and placement on it of a few glass microbeads (10–30 μm in diameter). In all the experiments, the otic capsule hole was covered with a window, fashioned from slide coverslip glass, to minimize motion of the perilymph meniscus overlying the recording site. BM vibrations were recorded by reflecting the beam of a laser velocimeter from the glass microbeads. The velocimeter consisted of a 20-mW He–Ne laser (Spectra Physics 106-1), a fiber vibrometer (Dantec 41X60), and a Doppler frequency tracker (Dantec 55n20.) The velocimeter was coupled to a compound microscope (Olympus BHMJ) equipped with 5 \times and 20 \times ultralong working distance objectives (Mitutoyo Plan Apo 5 \times , N.A. 0.14, and 20 \times , N.A. 0.42). The electrical output of the Doppler frequency tracker, a voltage proportional to the velocity, was filtered with a band-pass frequency response (1–15,000 Hz). The output of the filter was sampled by a computer at a rate of 100 kHz using a 16-bit A/D system (TDT AD1).

Acoustic stimuli were delivered via a Beyer DT-48 earphone. Stimuli consisted of tones, clicks, and analog Gaussian white noise. At the beginning of each experiment, the levels of acoustic tones were calibrated with a probe microphone with its tip positioned within 2 mm of the tympanic membrane. The noise stimuli were produced with a General Radio 1381 generator (20-kHz bandwidth) coupled to the earphone via an electronic switch (TDT SW1). Noise levels were measured using a spectrum analyzer and expressed in dB SPL/ $\sqrt{\text{Hz}}$ using the acoustic tone calibration. For Wiener kernel estimation, 100-ms analog noise bursts were presented every 400 ms. Stimulation with “frozen” noise was carried out using a single 10-ms analog noise burst previously digitized (TDT AD1) at a rate of 100,000/s and stored in computer memory. Frozen noise samples were presented every 100 ms. Exceptionally, stimulation in cochlea L125 noise was carried out using a TDT WG1 generator. In this case, the stimulation was continuous (duration=4 min) and BM response was sampled using a digital tape recorder (Sony DTC-690).

Wiener kernel analysis

For many nonlinear systems, the relationship between the input $x(t)$ and output $y(t)$ can be expressed via a sum of functionals (Marmarelis and Marmarelis 1978):

$$y(t) = \sum_{i=0}^{\infty} G_i[h_i, x(t)] \quad (1)$$

where $h_i(t)$ represents the i th Wiener kernel. The zeroth functional $G_0[h_0, x(t)]$, equals a constant and is

zero in the case of BM motion measured with a velocimeter. The first functional is determined by the convolution of the input with the first-order Wiener kernel (Marmarelis and Marmarelis 1978):

$$G_1[h_1, x(t)] = \int_0^{\infty} h_1(\tau)x(t-\tau)d\tau. \quad (2)$$

First-order Wiener kernels were estimated by cross-correlating the input noise, $x(t)$, to the BM velocity response, $y(t)$, in the frequency domain:

$$\Phi_{yx}(\omega) = X^*(\omega)Y(\omega). \quad (3)$$

The estimate of the first-order kernel, $h_1(\tau)$, is proportional to the inverse transform of $\Phi_{yx}(\omega)$:

$$h_1(\tau) = (1/P)\phi_{yx}(\tau). \quad (4)$$

P in Eq. 4 represents the power spectral density of the noise stimulus. Each kernel presented in this paper represents the average of at least 512 kernels (i.e., $h_1(\tau) = \frac{1}{N} \sum_{i=1}^N h_1^i(\tau)$). Equation 4 shows that the first-order kernel is proportional to the cross-correlation function computed from the input/output data. If the system is linear, the cross-correlation function remains the same across different stimulus levels. In the case of nonlinear systems, cross-correlation functions typically vary with stimulus level, but there are exceptions (Ringach and Shapley 2004).

In the present paper, we show that the first-order Wiener functionals (Eq. 2) can be used to predict BM responses to frozen noise. The first-order functionals can be thought of as the response of a linear system—with impulse response $h_1(t)$ —to the input $x(t)$ (Schetzen 1989). In other words, although $h_1(t)$ can have contributions from higher order odd nonlinearities, the first-order functional represents a linear approximation to the system at a given stimulus level. Equation 2 was implemented using the convolution function (*conv*) available in MATLAB®.

Computation of the envelopes and instantaneous frequencies of Wiener kernels and responses to clicks

The envelopes (Figs. 1C, D, 2B, 3B, 8C, D, and 9C, D) and instantaneous frequencies (Figs. 1E, F, 2C, 3C, 8E, F, and 9E, F) of responses to noise, first-order Wiener kernels, and responses to clicks were estimated using their analytic signal representation (Bennett 1970). The analytic signal of a waveform is a complex quantity whose real part is the waveform itself and whose imaginary part is the Hilbert transform of the real part. The envelope of the waveform is equal to the magnitude of the analytic signal and the instantaneous frequency corresponds to the derivative of the phase (insets in Figs. 2C and 3C) of the analytic signal.

RESULTS

BM responses to noise were recorded in seven chinchilla cochleae at basal sites with characteristic frequencies (CFs) in the 8- to 10-kHz range. CFs were estimated from BM responses to single tones recorded at the beginning of the experiment.

Waveforms of BM responses to Gaussian noise

Figure 1A, B shows average responses to frozen Gaussian white noise samples at BM sites in two cochleae with CFs of 9 kHz. Response waveforms are not broadband: at low stimulus levels (red dashed lines), inspection of the waveforms reveals periodicities with a frequency similar to CF (e.g., around nine cycles in 1 ms). This is expected for noise passing through a relatively narrow linear filter (p. 189 of Rice 1954). Figure 1A shows responses to frozen noise with levels differing by 40 dB recorded at the same BM site. The response to the weaker stimulus (red trace) was amplified 100 times (40 dB) to permit direct comparison of its gain (velocity per unit of pressure) with that for the response to the more intense stimulus (black trace). Should the BM vibrate linearly, the two traces would be identical. In fact, response waveforms are different: the response envelopes are not the same, gain is larger for the lower level noise, and the carrier frequencies are higher, on average, for the lower level noise.

Figure 1C shows the envelopes of the “raw” (i.e., unscaled) responses to the 25- and 65-dB noises shown (after scaling) in panel A and, additionally, of responses to 45-dB noise. In spite of using the same noise waveforms as stimulus for all the data shown in Figure 1, individual envelope oscillations vary substantially across levels, probably as a consequence of level-dependent changes in BM tuning. It is also apparent that the root mean square values of the envelopes grow at compressive rates, i.e., lower than 1 dB per decibel of increase of the stimulus level. Figure 1E shows the instantaneous frequencies corresponding to the traces of panel A. Frequencies are higher for the responses to the 25-dB stimuli than for 65-dB stimuli, also probably as a consequence of level-dependent changes in tuning.

Figure 1B, D, and F presents waveforms and analyses similar to those of panels A, C, and E, but for responses recorded from another cochlea to otherwise identical noise samples with levels differing by 50 dB. In this case, the trace in panel B corresponding to the response to the weaker stimulus was amplified 317 times (i.e., 50 dB) to facilitate comparison with the more intense stimulus. In all respects, the analyses of the responses are similar to those seen above in panels A, C and E, exhibiting the

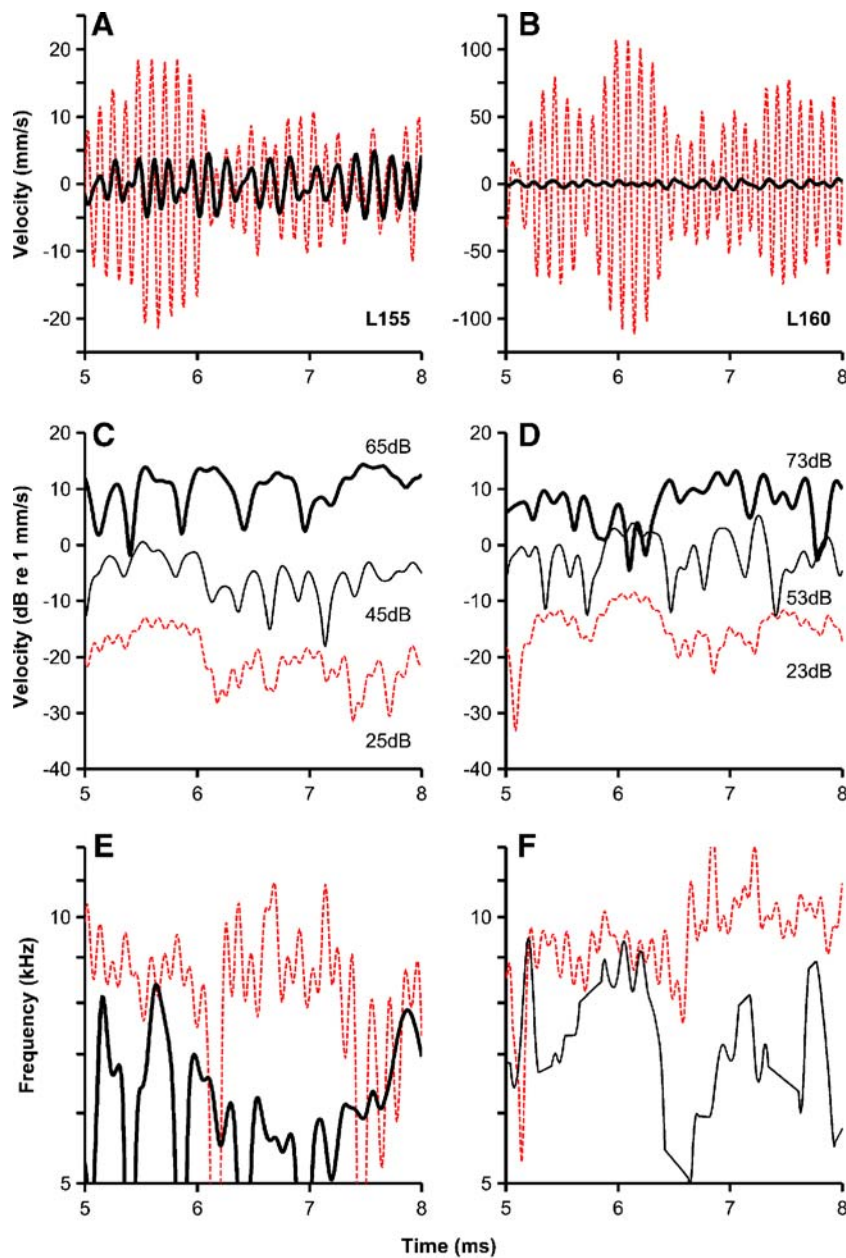


FIG. 1. Waveforms (*top panels*), envelope magnitudes (*middle panels*), and instantaneous frequencies (*bottom panels*) of BM responses to noise. **A** Average BM responses to multiple repetitions of frozen noise samples at 65 dB SPL/√Hz (*black lines*) and 25 dB SPL/√Hz (*red lines*). Responses to the 25-dB noise sample were multiplied by 100 (i.e., scaled up by 40 dB so that they are comparable to the responses to the 65-dB noise). **B** Average BM responses to multiple repetitions of frozen noise samples at 73 dB

SPL/√Hz (*black lines*) and 23 dB SPL/√Hz (*red lines*). Responses to the 23-dB noise sample were multiplied by 317 (i.e., scaled up by 50 dB so that they are comparable to the responses to the 73-dB noise). **C, D** Raw (unscaled) magnitudes of the response envelopes of the waveforms in **A** and **B**, respectively. Also shown are magnitudes of response envelopes to 45-dB (**C**) and 53-dB (**D**) noise samples. **E, F** Instantaneous frequencies of the waveforms in **A** and **B**, respectively.

same signs of nonlinearity: compression and spectral shifts toward lower frequencies as a function of increasing stimulus level.

Spectral analysis of responses to noise is usually performed on the autocorrelation function of the response. The resulting power spectrum contains information about frequency tuning, but not about phases. Therefore, analysis of BM responses to noise was carried

out using first-order Wiener kernels, cross-correlograms of the input noises and the corresponding responses, which preserve phase information.

First-order Wiener kernels: time domain analysis

Figure 2A illustrates the first-order Wiener kernels, $h_1(t)$, of BM responses to white Gaussian noise (not frozen)

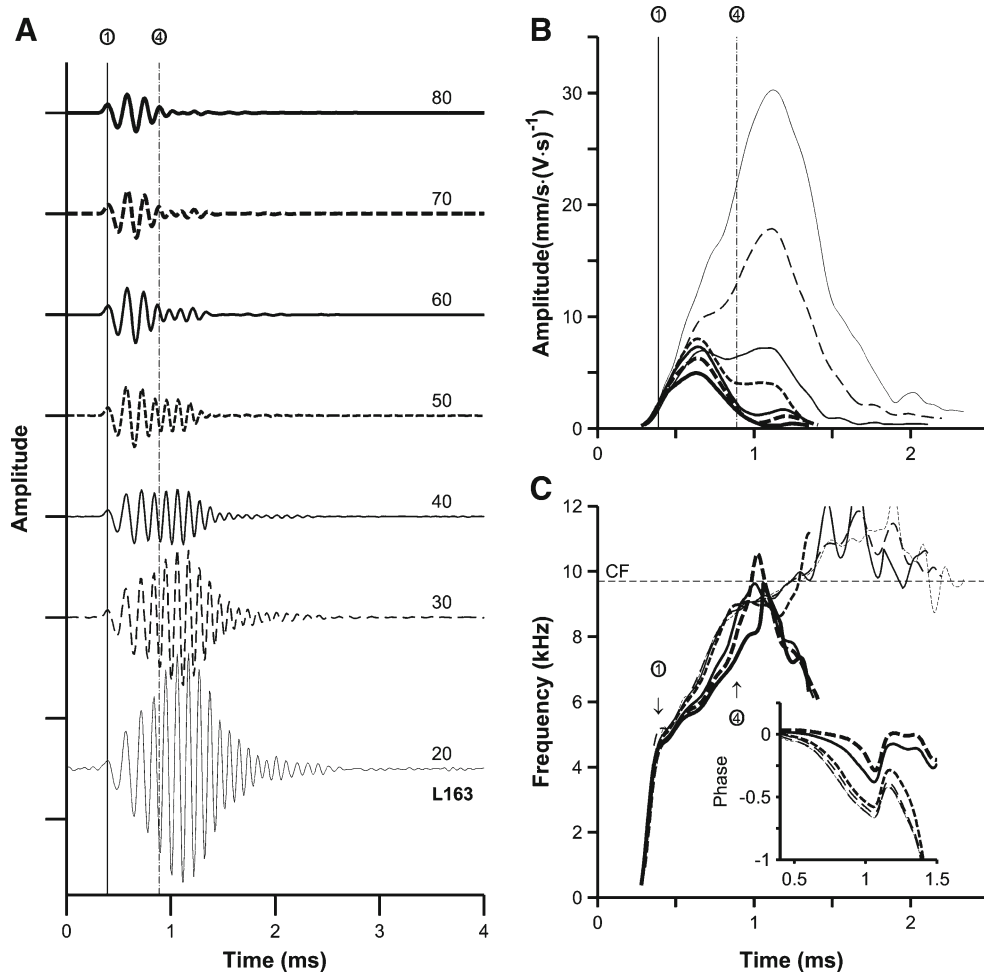


FIG. 2. First-order Wiener kernels for BM responses to noise and their analytic signal representations. **A** Waveforms of first-order Wiener kernels for responses to noise presented at the indicated levels. The vertical lines indicate the first and fourth peaks of responses to intense stimuli. **B** Envelopes of kernels. Note that the

envelopes are the magnitudes of the analytic signal. **C** Main, instantaneous frequencies of kernels. Inset, phases (in periods) of the analytical signals, plotted relative to the phases for the 80-dB stimulus. Note that instantaneous frequencies are the slopes of the phases. Stimulus levels are expressed in dB SPL/ $\sqrt{\text{Hz}}$.

presented at several stimulus levels. For low stimulus levels, the waveforms consist of lightly damped oscillations characteristic of narrowly tuned band-pass systems. If BM vibrations were linear, the amplitude and shape of the Wiener kernels would be identical regardless of stimulus level. In fact, both the shapes and magnitudes of the waveforms change systematically with level. The amplitude and time of occurrence of the first oscillation peaks—marked with a thin continuous line across levels—remain nearly constant (Fig. 2A, B), but later oscillations decrease in size as the stimulus level increases. The time of occurrence of some of the later oscillations also vary across stimulus levels. For example, the time of the fourth oscillation peak of the 80-dB kernel (dot-and-dash line) corresponds approximately to zero crossings in the 50- and 60-dB kernels and to the fourth trough in the 20-dB kernel. Such a change corresponds to a phase shift amounting to a 180-degree phase lag relative to the first positive peak.

Figure 2B displays the envelopes of the kernels computed using their analytic signal representations (see “Methods”). All the envelopes have similar values near their onsets (<0.5 ms), but decrease in magnitude at later times as a function of increasing stimulus level. This indicates that whereas the first oscillations of the kernels grow linearly, later oscillations do not. Figure 2C shows the phases of the analytic signal (inset) and their slopes (i.e., instantaneous frequencies), in the main panel, for the kernels of Figure 2A. The instantaneous frequencies first increase systematically as a function of time and then fluctuate around CF. Such frequency modulation is consistent with the phase changes noted in Figure 2A. Note also that the curves are not constant across levels either, except for times <0.5 ms. The phases and the instantaneous frequency curves are steepest and similar to each other for responses to noise presented at 20–50 dB SPL. The slopes decrease systematically with level between 50 and 80 dB SPL. Again, this is consistent

with the changes across levels in peak times in the waveforms depicted in Figure 2A.

Figure 3 shows the results of an analysis similar to the one illustrated in Figure 2 but for a different cochlea. All of the main features of the Wiener kernels noted for Figure 2, including the different rates of growth of the first vs. later peaks, the decreasing envelope magnitudes as a function of level, the presence of frequency (or phase) glides, and the decrease of their slopes with increasing stimulus level, are also present in Figure 3.

First-order kernels were also obtained for middle ear vibrations in some chinchillas. Figure 4A shows the first-order Wiener kernel (black continuous line) and the response to clicks (red dashed line) measured near the incudo-stapedial junction. Consistent with the linearity of the middle ear responses, both waveforms are very similar. A first-order kernel obtained for BM responses in the same chinchilla is shown in Figure 4B. A vertical red line in Figure 4B indicates the time at which the first oscillation of the stapes kernel (Fig. 4A) reaches 20% of its peak value. Using the same criterion (20% of the first response maximum), BM motion begins about 38 μ s after the onset of ossicular vibration.

First-order Wiener kernels: frequency analysis

Figure 5A, B shows the Fourier transform amplitudes of the time waveforms of Figures 2A and 3A, respectively. The CFs of the preparations (dots) were 9.7 and 9 kHz, respectively. Because computation of the first-order kernels involves normalization to the noise level, the plots in Figure 5A, B can be considered as estimates of BM gain. For frequencies well below CF, gain values are the same regardless of stimulus level. Around CF, however, gain increases as the stimulus level decreases.

Regardless of noise input level, all the amplitude–frequency curves of Figure 5 have band-pass shape. For the lowest stimulus level, the peak of the response coincides with the CF measured from responses to tones. For the highest stimulus levels, the peak gains occur at frequencies 0.64 and 0.5 octaves lower than CF. An estimate of the gain of the “cochlear amplifier” can be obtained by subtracting the peak of the response to the most intense noise from the peak (at CF) in the response to the lowest level noise. Such estimates of the cochlear-amplifier gain were 18 and 22 dB for the data shown in Figure 5A, B, respectively. A different measure of cochlear amplification is obtained if the gain subtraction is performed at CF. Measured that way, cochlear amplification amounted to 47 and 28 dB for the data of Figure 5A, B, respectively. Frequency selectivity of the kernels was quantified using the “quality factor,” $Q_{10\text{dB}} = \text{BF} / (\text{bandwidth at } 10 \text{ dB re BF response})$, where BF is the best frequency, the stimulus frequency which evokes the most sensitive responses,

without regard to stimulus level or physiological state (CF is the BF in normal cochleae at the lowest effective stimulus levels). The results indicate that frequency selectivity decreases as a function of stimulus level [L163: $Q_{10\text{dB}}(20 \text{ dB SPL}) = 2.8$, $Q_{10\text{dB}}(80 \text{ dB SPL}) = 1.55$. L155: $Q_{10\text{dB}}(20 \text{ dB SPL}) = 1.90$, $Q_{10\text{dB}}(70 \text{ dB SPL}) = 1.35$]. These $Q_{10\text{dB}}$ values are similar to those for responses to tones. For example, for chinchilla L113 (Fig. 9 in Ruggero et al. 1997), $Q_{10\text{dB}}(30 \text{ dB SPL}) \approx 3.33$ and $Q_{10\text{dB}}(80 \text{ dB SPL}) \approx 1.1$.

Figure 5A also shows the gains (i.e., response amplitudes normalized to stimulus level) of BM responses to CF tones (open circles). The slopes of the corresponding amplitude–level curve were as low as 0.08 dB/dB in the 30- to 60-dB SPL range. To facilitate comparison with the responses to noise, the gain of the response to the CF tone presented at 10 dB SPL was shifted arbitrarily to match the Wiener kernel responses at 20 dB SPL/ $\sqrt{\text{Hz}}$, and then responses to 20–70 dB SPL tones, in steps of 10 dB SPL, were shifted by the same amount. The response gains for 10–60 dB SPL tones matched the Wiener kernels very well.

Figures 6A and 7A display the phase-vs.-frequency functions of the Fourier transforms of the Wiener kernels measured at several stimulus levels. Again, if the system was linear, all the phase functions would overlap. In fact, phases were level-dependent. Variation of the phase-vs.-frequency curves as a function of stimulus level can be observed in greater detail by plotting phase functions relative to the phases of the kernel obtained with the highest level stimulus (Figs. 6B and 7B). For frequencies lower (higher) than a certain value higher than CF, there is an increase (decrease) in phase lag with increasing stimulus level. Maximum phase lags occur at frequencies approximately equal to (Fig. 6B), or somewhat higher than (Fig. 7B), CF (dots). The frequencies at which phase shifts equal zero are usually higher than CF.

Comparison of BM first-order Wiener kernels and responses to clicks

Figures 8 and 9 allow for comparisons of first-order Wiener kernels (black lines) and responses to rarefaction clicks recorded at the same BM sites in the same chinchilla cochleae (red lines). The levels of the noise stimuli are indicated in each panel. In each figure, responses to lower level clicks (Figs. 8B and 9B) were multiplied by the same scaling factor determined by matching the Wiener kernels and the responses to clicks for the higher level stimuli (Figs. 8A and 9A). To verify that the physiological state of the cochlea was stable, BM responses to clicks and/or responses to CF tones were measured before and after the noise experiments. No significant differences were detected, indicating no deterioration in the intervening period.

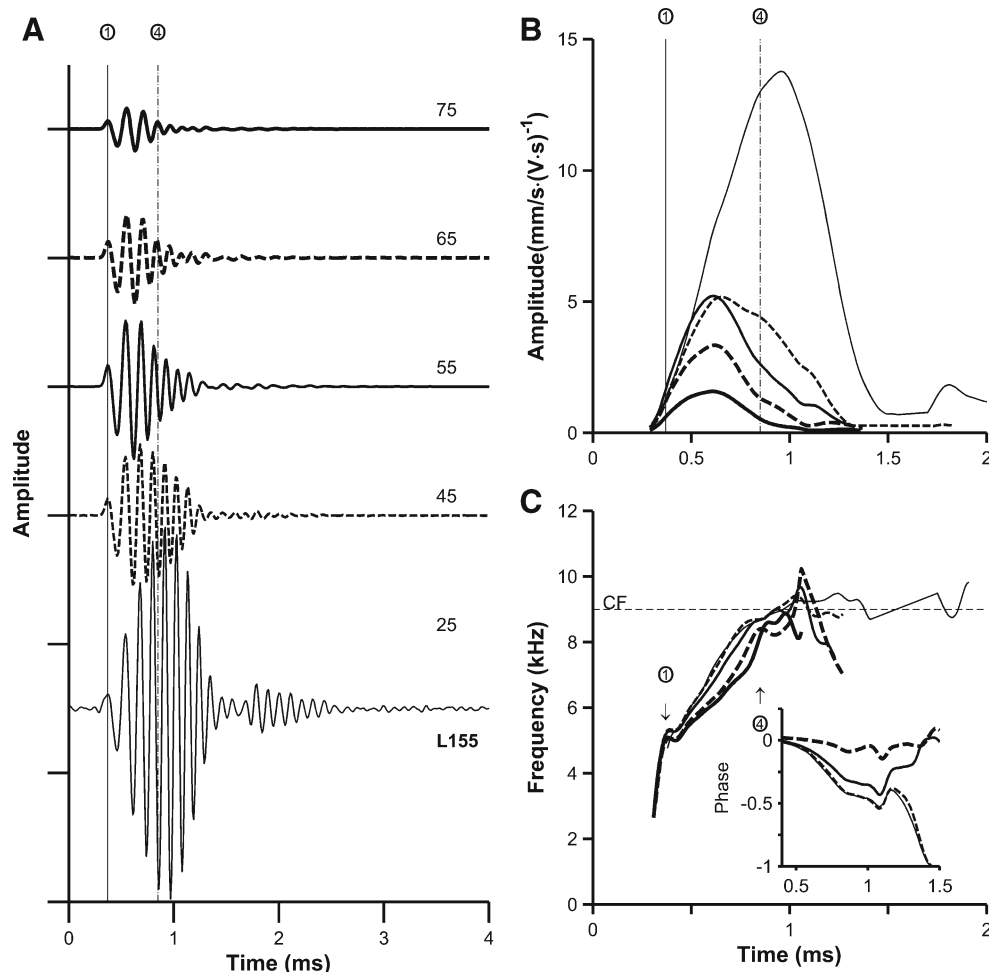


FIG. 3. First-order Wiener kernels for BM responses to noise and their analytic signal representations. Analyses as in Figure 2 but for recordings in a different chinchilla cochlea. *Inset of C*, phases of the analytical signals, plotted relative to the phases for the 75-dB stimulus.

Panels A and B of Figures 8 and 9 show that although the main lobes of the time domain responses to clicks and kernels are nearly identical, responses to clicks last longer than the corresponding kernels, i.e., responses to clicks are more sharply tuned than the Wiener kernels. This can be seen especially well by comparing the envelope of first-order kernels (black lines in Figs. 8C, D and 9C, D) and BM click responses (red lines in Figs. 8C, D and 9C, D; note that envelope values are plotted only if they exceed 10% of the peak values). Instantaneous frequency-vs.-time functions are the same for kernels and BM click responses (Figs. 8E, F and 9E, F), but last longer (i.e., the envelope values were above noise level) for BM click responses. Differences between kernels and responses to clicks were less obvious for lower stimulus level, probably due to low signal-to-noise ratios of the recordings.

BM responses to noise predicted by first-order Wiener kernels

Figure 10 shows segments of average BM responses (red dashed lines) in two cochleae to identical

repetitions of a short sample of white Gaussian noise (frozen noise) and responses predicted by first-order Wiener functionals (black continuous lines). For each cochlea, responses are shown for stimuli presented at two levels (panels A and C for L155, B and D for L160). The Wiener functionals were computed by convolving the frozen noise stimuli with the first-order Wiener kernels obtained using longer and different white noises but with the same spectral level. The predicted responses were nearly identical to the measured responses. The accuracy of the predictions was quantified using the correlation coefficient: $\rho=0.93$, 0.96 , 0.97 , and 0.95 for the results in Figure 10A–D, respectively. The square of the correlation coefficients (pp. 33 and 34 in Draper and Smith 1981) indicate that predictions by first-order Wiener functionals account for most of the variance of the measurements: 87% ($=100 \rho^2$), 91%, 94%, and 90% in Figure 10A–D, respectively. Thus, in spite of the compressive nonlinear behavior evident in the waveforms of responses to noise (Figs. 1 and 10) and in first-order Wiener kernels (Figs. 2, 3, 5, 6, 7), BM responses to noise are predicted very well by linear filtering.

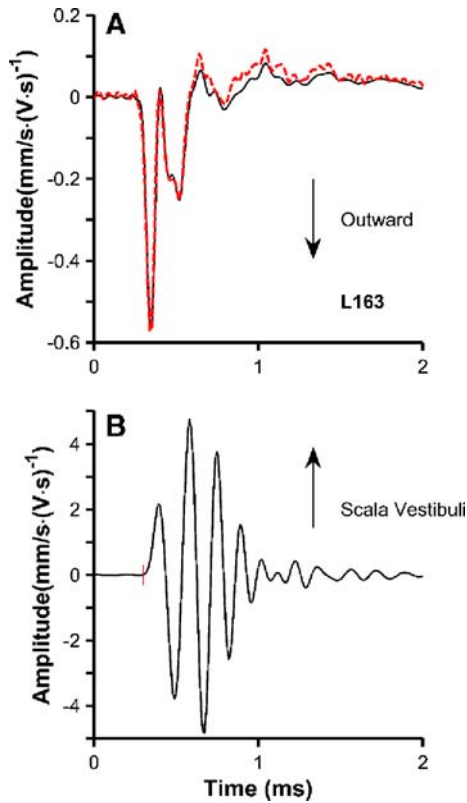


FIG. 4. First-order Wiener kernels of middle ear and BM responses to noise recorded in the same ear. Also shown are middle ear responses to clicks (**A**). **A** Responses to rarefaction clicks (*red dashed line*) and first-order kernel of stapes responses to noise (*continuous black line*). Negative polarity indicates motion away (outward) from oval window. **B** First-order kernel of BM responses to 80-dB noise. Positive polarity indicates velocity towards scala vestibuli. *Red vertical line* indicates the onset of stapes vibration.

Statistical distributions of BM responses to noise

The statistical distribution of BM responses to frozen noise samples was determined in several preparations. Figure 11A–D shows cumulative probability distribution functions (CDFs) computed for normalized BM responses to noise in two cochleae (continuous lines). For comparison, Figure 11 also shows the CDFs (dashed lines) of a standard Gaussian random variable with the same mean ($\mu=0$) and standard deviation ($\sigma=1$) as the normalized BM data. The empirical and theoretical CDFs are very similar. This result was verified using a one-sample Kolmogorov–Smirnov test (MATLAB®).

A statistical analysis was also performed on the envelope functions of BM responses to frozen noise samples. Standard deviations (σ) of the envelope fluctuations expressed in decibels (Fig. 1C, D) change only minimally across stimulus level (L155: $\sigma_{65\text{dB}}=5.49$, $\sigma_{45\text{dB}}=4.64$, and $\sigma_{25\text{dB}}=4.43$ dB re 1 mm/s; L160:

$\sigma_{73\text{dB}}=5.24$, $\sigma_{53\text{dB}}=4.7$, and $\sigma_{23\text{dB}}=4.68$ dB re 1 mm/s). Empirical CDFs of the envelope fluctuation are shown in the insets in Figure 11A, B together with theoretical CDFs of a Rayleigh distribution, i.e., the distribution of the envelope fluctuations of a band-pass Gaussian process (Papoulis 1984). Again, the empirical and theoretical CDFs are very similar. The similarities between the statistical properties of Gaussian white noise and the BM responses shown in Figure 11 are consistent with the fact that linear filtering accurately predicts BM responses to noise, provided that both the linear filters (i.e., the first-order Wiener kernels) and the predicted responses are for same-level stimuli (Fig. 10).

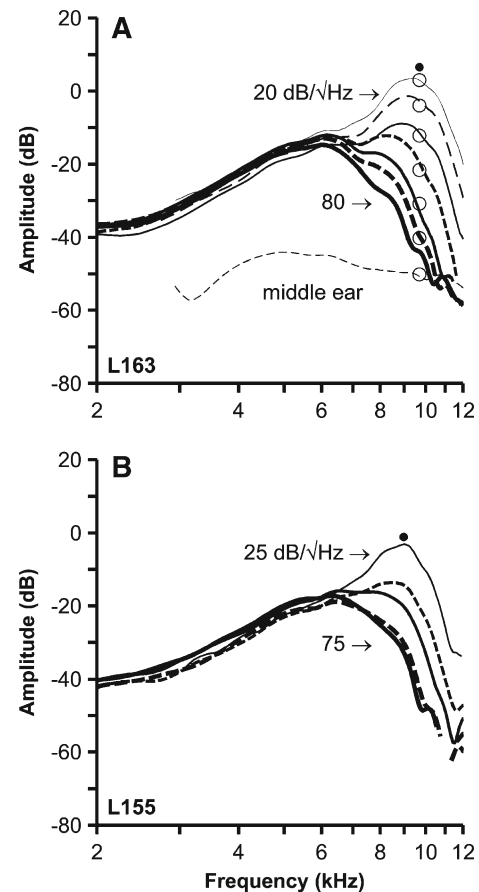


FIG. 5. Magnitude spectra of first-order Wiener kernels. *Dots* indicate CF. **A** Fourier transform amplitudes of BM kernels shown in Figure 2A and middle ear responses of Figure 4A. *Open symbols* indicate relative gains (i.e., velocity normalized to stimulus level) of responses to CF tones presented at 10, 20, 30, 40, 50, 60, and 70 dB SPL. Gains for responses to tones presented at 10 dB SPL were equated to those of Wiener kernels for responses to noise presented at 20 dB SPL/√Hz. 0 dB for ordinate scale corresponds to 1 (mm/s)·(V s)⁻¹ for Wiener kernels. **B** Fourier transform amplitudes of kernels shown in Figure 3A. 0 dB for ordinate scale corresponds to 1 (mm/s)·(V s)⁻¹.

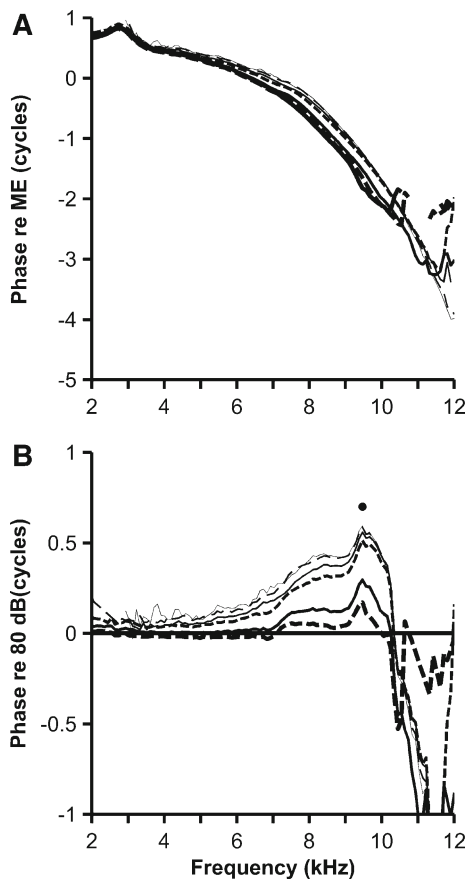


FIG. 6. Phases of first-order Wiener kernels re middle ear ossicular vibrations. Analyses for the cochlea illustrated in Figure 2. *Thick black lines (horizontal in B)* correspond to kernels obtained using 80-dB noise stimuli. *Other lines* indicate phases from kernels computed using weaker stimuli (70, 60, 50, 40, 30, and 20 dB SPL/ $\sqrt{\text{Hz}}$). **A** Phase values correspond to BM velocity toward scala vestibuli relative to stapes outward velocity. **B** Phases relative to phases of 80-dB kernel. Positive phase values correspond to phase leads. *Dot* indicates CF.

SUMMARY AND DISCUSSION

Summary of findings

1. The waveforms of BM responses to noise exhibit level-dependent compressive nonlinearities similar to those that characterize responses to tones and clicks.
2. Both the zero crossing times and the onset frequency glides of first-order Wiener kernels of responses to noise vary with stimulus level.
3. First-order kernels closely resemble BM responses to clicks. However, responses to clicks “ring” longer than Wiener kernels.
4. The statistical distribution of BM responses to Gaussian white noise is also Gaussian and the envelopes of the BM responses are Rayleigh distributed, as they should be for band-pass Gaussian noise.

5. At any given stimulus level, BM responses to noise are well approximated by a linear filter with impulse response specified by the first-order Wiener kernel computed from responses to noise of the same level.

Comparison of BM first-order Wiener kernels in chinchilla and guinea pig

The present use of first-order Wiener kernels to analyze BM responses to noise has a precedent in a series of similar studies in guinea pig (de Boer and Nuttall 1997, 2000). In general, Wiener kernels in chinchilla resemble those in guinea pig. However, whereas the studies in guinea pig emphasized the preservation of zero crossing times (and, hence, of frequency “glides”) across stimulus levels, the present results show that zero crossing times (Figs. 2A and 3A) and frequency glides (Figs. 2C and 3C) in chinchilla

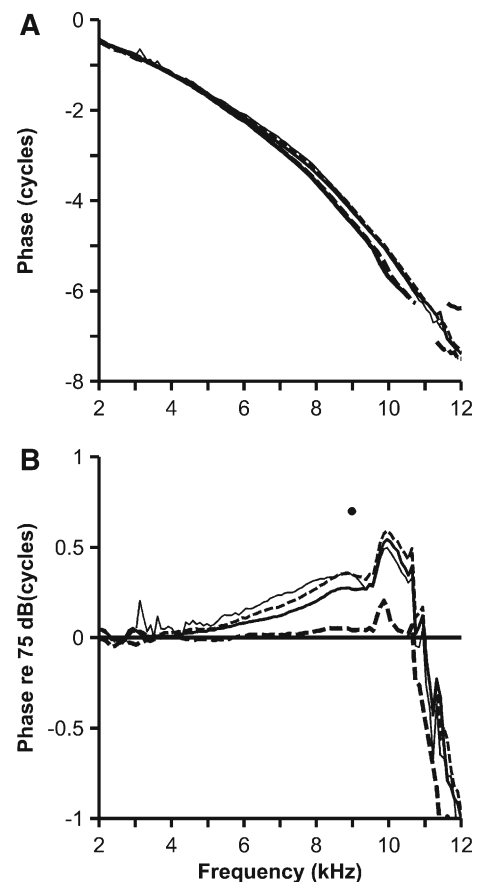


FIG. 7. Phases of first-order Wiener kernels. Analyses for the cochlea illustrated in Figure 3. Phases correspond to BM velocity toward scala vestibuli relative to the electrical stimulus (middle ear vibrations were not measured). *Thick lines (horizontal in B)* indicate responses to 75-dB stimuli. *Other lines* represent phases from kernels computed using lower level stimuli (65, 55, 45 and 25 dB SPL/ $\sqrt{\text{Hz}}$). Other details as in Figure 6.

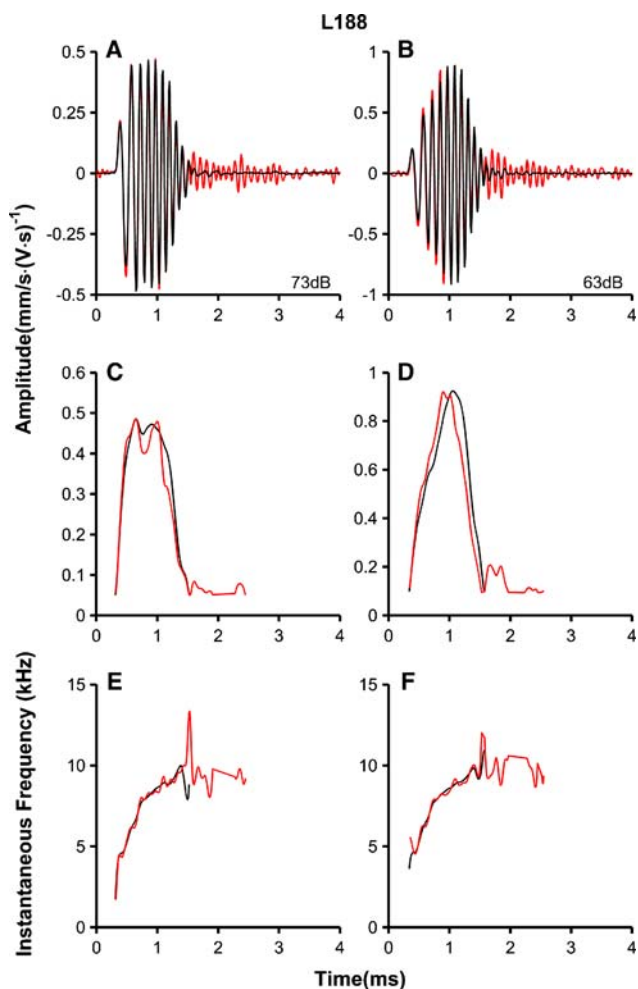


FIG. 8. Comparisons of first-order Wiener kernels and responses to clicks measured in the same cochlea. *Black lines* indicate first-order Wiener kernels for responses to noise presented at the indicated levels. Clicks were presented at 88 (A) and 78 (B) dB peak SPL. *Red lines* indicate averages of responses to 512 10- μ s clicks presented every 51 ms. **C, D** The response envelopes (only for values that exceed 10% of the peak). **E, F** Instantaneous frequency-vs.-time functions.

kernels vary systematically with stimulus level. The contrast between the level dependence of frequency glides in Wiener kernels of responses to noise in chinchilla and their apparent independence in guinea pig might conceivably reflect species differences. However, that possibility seems ruled out by the level dependence of zero crossings in guinea pig BM responses to clicks (see Fig. 6 of Guinan and Cooper 2008). Another possibility is differences between the physiological states of the cochleae in which the contrasting results were obtained. Changes in kernel spectral magnitude across intensity levels were smaller in guinea pig than in chinchilla: compare the magnitude change, 47 dB, between CF responses to 20- and 80-dB stimuli in Figure 5A vs. 20 dB in Fig. 1 of

de Boer and Nuttall (2000). This difference in compression suggests weaker amplification in the guinea pig cochleae and hence smaller changes in frequency and timing than in the present data.

Comparison between BM Wiener kernels and responses to clicks or tones

In general, the features of first-order Wiener kernels of chinchilla BM responses to noise, including the level dependence of frequency glides, closely resemble counterparts in responses to clicks (Figs. 8 and 9). Variation of zero crossings and glide slopes across stimulus levels is evident (albeit not always explicitly acknowledged) in illustrations of BM responses to clicks in chinchilla (Recio et al. 1998; Recio and Rhode 2000) and guinea pig (Guinan and Cooper 2008). The level dependencies of glides in Wiener kernels (Figs. 2C and 3C) and chinchilla BM

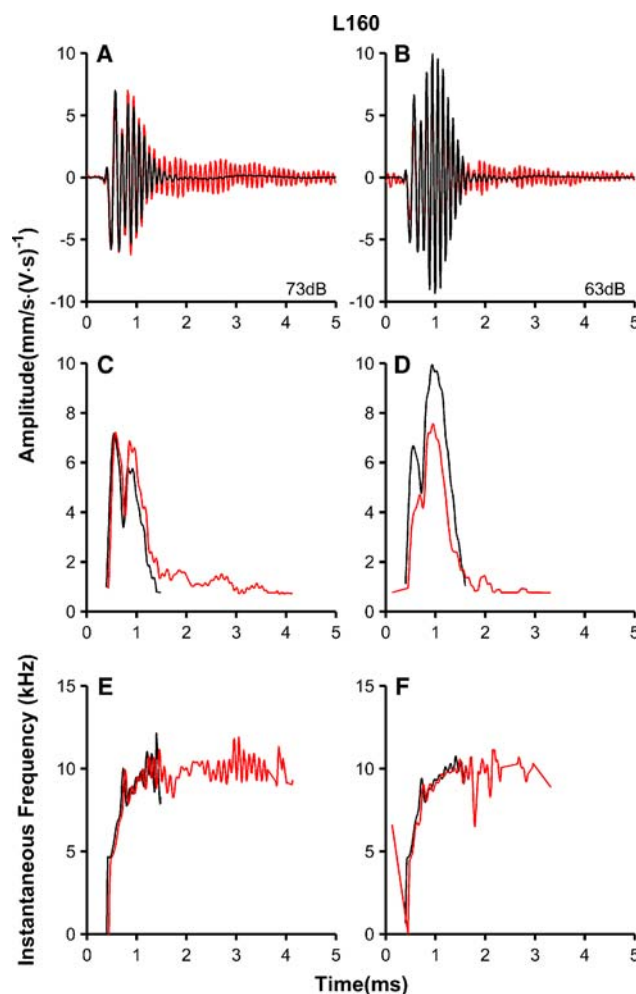


FIG. 9. Comparisons of first-order Wiener kernels and responses to clicks measured in the same cochlea. Same analyses as in Figure 8, but for a different cochlea. Clicks were presented at 84 (A) and 74 (B) peak SPL.

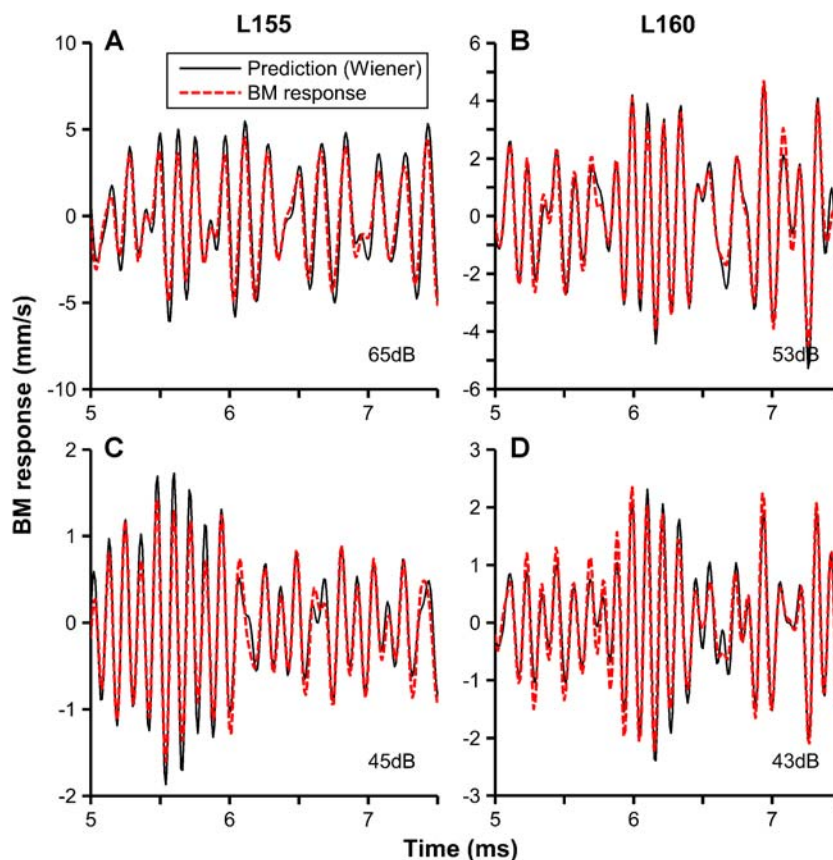


FIG. 10. Prediction of BM responses to noise using first-order Wiener kernels. *Dashed red lines* indicate BM responses to frozen white noise stimuli in two cochleae (L155 in **A** and **C**; L160 in **B** and **D**). Noise level is indicated in **A**, **C**, **B**, and **D**. *Continuous black lines*

indicate the output of a linear filter whose impulse response is the first-order Wiener kernel obtained from different noise stimuli of the same level. Input to the linear filter is the stimulus used to evoke BM responses.

responses to clicks (Fig. 6A of Recio et al. 1998) are similar in that slopes are steep for low- and moderate-level stimuli and shallower for intense stimuli. A corresponding distinction is observable in the zero crossings of guinea pig BM responses to low- and high-level clicks (Fig. 6 of Guinan and Cooper 2008). The intensity dependencies of phases are qualitatively similar in kernels and BM responses to clicks (Recio et al. 1998) and tones (Ruggero et al. 1997). However, the intensity-dependent phase variations at CF appear to be larger in Wiener kernels (compare Figs. 6B and 7B with Fig. 15 in Recio et al. 1998, Fig. 10 in Ruggero et al. 1997, and Fig. 2F in Rhode and Recio 2000).

The most salient difference between Wiener kernels and responses of clicks is that the latter exhibit an extra-long narrowband oscillation not present in the kernels of responses to noise recorded in the same cochleae (Figs. 8 and 9). Similar differences exist between BM responses to clicks and “synthetic impulse responses” obtained by inverse Fourier transformation of BM responses to tones (Recio and Rhode 2000). One explanation for the extra-long ringing in responses to clicks is the possible existence of a time-dependent cochlear nonlinearity (p. 3585 of

de Boer and Nuttall 1997). The effects of such nonlinearity should be strong in the case of clicks because of their punctate temporal nature, but mild in the case of constant-level noise or tones. This subject is further addressed below, in “Explanation of the coexistence of quasi-linear and nonlinear properties in BM responses to noise” of the discussion.

Level dependence and vulnerability of frequency glides in relation to cochlear tuning

Even though several studies emphasized the apparent invariance of frequency glides (Carney et al. 1999; de Boer and Nuttall 2000; Shera 2001; Tan and Carney 2003), the present results and others on responses to clicks (Guinan and Cooper 2008; Recio et al. 1998; Recio and Rhode 2000) show that frequency glides, much as other aspects of cochlear mechanics, are actually level-dependent (i.e., nonlinear) *in vivo*. In chinchilla, the frequency glides of responses to clicks also depend on the physiological state of the cochlea, since their slopes are lowest postmortem [see Fig. 6 of Recio et al. 1998]. The specific dependence of the frequency glides on stimulus level and on the

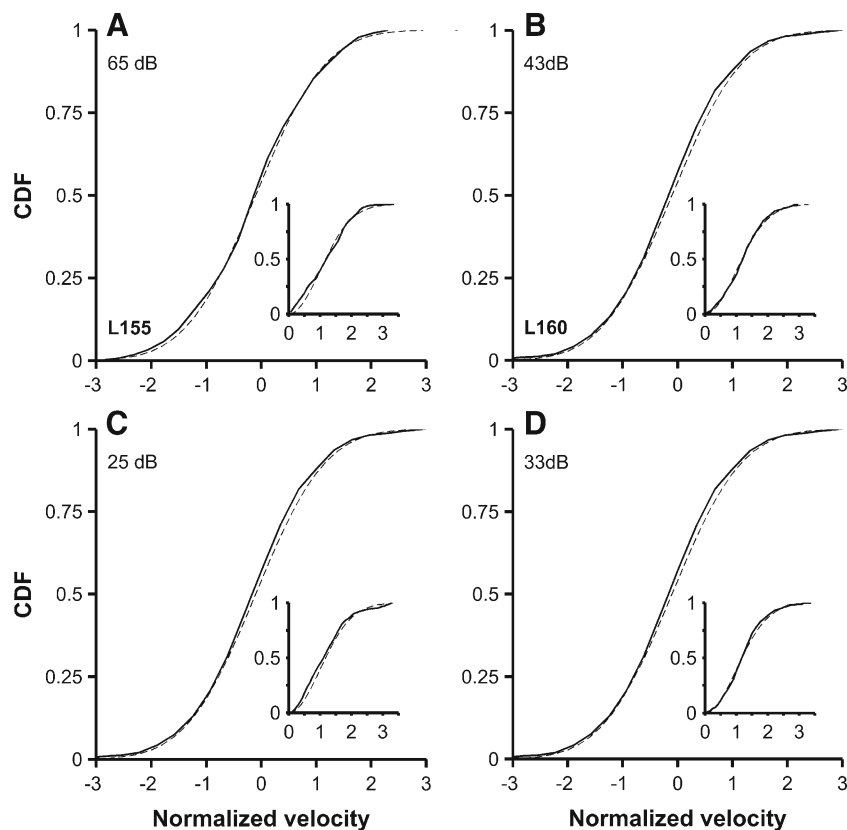


FIG. 11. Cumulative probability distribution functions (CDFs) of BM responses to frozen noise. Stimulus levels are indicated in each panel. *Continuous lines* in the main graphs represent the CDFs obtained from the normalized BM responses ($\mu=0$, $\sigma=1$) in same two

cochleae represented in Figure 1 (L155 in **A** and **C**; L160 in **B** and **D**). *Dashed lines* indicate the CDFs of standard Gaussian variables. *Insets* indicate empirical (*continuous lines*) and Rayleigh (*dashed lines*) CDFs of the BM response envelopes.

physiological state of the cochlea—instantaneous frequency climbs rapidly toward CF in low-level responses, more slowly in high-level responses and even more slowly postmortem—seems consistent with the level-dependent changes in tuning, sharp and centered at CF for low stimulus levels vs. broad and centered at lower frequencies for high stimulus levels and postmortem. The level dependence of the frequency glides also seems consistent with the time course of amplification or compression. This may be appreciated by comparing the envelopes and the instantaneous frequencies of the Wiener kernels (panels B and C of Figs. 2 and 3), both of which rise at a faster rate for low-level responses.

In many systems, asymmetries in frequency tuning are associated with phase modulation (i.e., frequency glides) in impulse responses (pp. 131–132 of Papoulis 1962; p. 123 of Papoulis 1977). In the context of cochlear function, a connection between the asymmetries of cochlear tuning and of frequency glides has been recognized (p. 2292 of Recio and Rhode 2000; p. 210 of Lyon 1997; p. 2008 of Tan and Carney 2003). Further, a recent abstract (Temchin et al. 2009) claims that realistic phase–frequency curves and impulse responses with frequency glides of appropri-

ate polarity (high to low frequencies for CFs < 1 kHz and low to high frequencies for higher CFs) can be predicted from synthetic frequency–threshold tuning curves of auditory nerve fibers (Temchin et al. 2008). If that claim is confirmed, it will be of interest to ascertain whether realistic level-dependent frequency glides can also be predicted on the basis of the level-dependent variations of cochlear tuning.

Quasi-linear and nonlinear aspects of BM responses to noise

BM responses to noise exhibit the same type of cochlear nonlinearity which yields responses to tones with little harmonic distortion (Cooper 1998; Rhode 2007; Ruggero et al. 1997) in spite of enormous compression of response magnitudes (growth rates as low or lower than 0.1 dB/dB; Rhode 2007). On the one hand, responses to noise are quasi-linear in that first-order Wiener functionals predict the waveshapes of BM responses to noise with substantial accuracy (Fig. 10); their statistical distributions are Gaussian (Fig. 11), as they should be in linear systems (but not necessarily for nonlinear filters; Papoulis 1984), and their envelopes are Rayleigh distributed, as they

should be for band-pass Gaussian noise (Fig. 11, insets). On the other hand, the magnitudes of BM responses to noise exhibit highly compressive growth (Figs. 1, 2, and 3), comparable to the compressive growth of response to tones (Fig. 5). Quantitatively, the accuracy of the predictions of BM responses to noise based on first-order Wiener kernels seems consistent with the waveform distortion in BM responses to tones at basal sites of the cochlea, which consists mainly of second-order components amounting to <-28 dB relative to responses at the fundamental frequency (Cooper 1998) and typically -15 to -30 dB (but exceptionally as large as -6 dB) in chinchilla (Rhode 2007). Since the first-order Wiener kernels of nonlinear systems embody linear and, potentially, odd-order (but *not* even-order) system components, it is reasonable that the first-order Wiener functionals account for about 90% of the variance of responses to noise, the remaining 10% of the variance (i.e., -20 dB) presumably reflecting second-order harmonic distortion.

Explanation of the coexistence of quasi-linear and nonlinear properties in BM responses to noise

To explain why first-order Wiener kernels computed from responses to noise presented at any given level can so accurately predict BM responses to other noise samples presented at the same level, we adopt the argument put forth by Egbert de Boer in justifying his EQ-NL theorem (de Boer 1997). The key concept is that, for any given average level of stimulation, the active process produces a corresponding average amplification. Since the first-order Wiener kernel “can always be interpreted as the impulse response of a linear model” (de Boer 1997), the first-order Wiener kernel computed at any given level of stimulation is identical to the impulse responses of a *level-specific linear* model, which accurately predicts responses to other noise samples presented at the same level (but not others).

Implication of quasi-linear cochlear filtering in responses to wideband stimuli

The quasi-linear filtering of wideband inputs in the cochlea has implications for understanding the temporal processing of environmental and speech sounds, which are often wideband in nature. In particular, quasi-linear filtering contradicts the common assumption that cochlear processing can be validly modeled as a band-pass linear filter followed by an instantaneous nonlinearity (e.g., see Fig. 6 and pp. 356–357 of Oxenham and Bacon 2003). In contrast with quasi-linear filtering, such a model produces “envelope (fluctuation) compression” (com-

pare Fig. 1C or D with Fig. 5 of Oxenham and Bacon 2003). Quasi-linear filtering implies that BM nonlinearity is not instantaneous and suggests that cochlear processing involves time-consuming (albeit fast) automatic gain control (Lyon 1990; van der Heijden 2005; Zwislocki et al., 1997).

ACKNOWLEDGMENTS

We thank Andrei Temchin, Marcel van der Heijden, and Nigel Cooper for their many helpful comments on earlier versions of this manuscript. We were supported by NIH Grant DC-000419.

REFERENCES

- BENNETT WR. Introduction to Signal Transmission. New York, McGraw-Hill, 1970.
- CARNEY LH, MCDUFFY MJ, SHEKHTER I. Frequency glides in the impulse responses of auditory-nerve fibers. *J. Acoust. Soc. Am.* 105:2384–2391, 1999.
- CARNEY LH, YIN TC. Temporal coding of resonances by low-frequency auditory nerve fibers: single-fiber responses and a population model. *J. Neurophysiol.* 60:1653–1677, 1988.
- COOPER NP. Harmonic distortion on the basilar membrane in the basal turn of the guinea-pig cochlea. *J. Physiol.(Lond.)* 509(Pt 1):277–288, 1998.
- DE BOER E. Correlation studies applied to the frequency resolution of the cochlea. *J. Aud. Res.* 7:209–217, 1967.
- DE BOER E. Connecting frequency selectivity and nonlinear models of the cochlea. *Aud. Neurosci.* 3:377–388, 1997.
- DE BOER E, NUTTALL AL. The mechanical waveform of the basilar membrane. I. Frequency modulations (“glides”) in impulse responses and cross-correlation functions. *J. Acoust. Soc. Am.* 101:3583–3592, 1997.
- DE BOER E, NUTTALL AL. The mechanical waveform of the basilar membrane. III. Intensity effects. *J. Acoust. Soc. Am.* 107:1497–1507, 2000.
- DRAPER NR, SMITH H. Applied Regression Analysis. New York, Wiley, 1981.
- EVANS EF. Frequency selectivity at high signal levels of single units in cochlear nerve and nucleus. In: Evans EF, Wilson JP (eds) *Psychophysics and Physiology of Hearing*. London, Academic, pp. 185–192, 1977.
- GUINAN JJ, JR, COOPER NP. Medial olivocochlear efferent inhibition of basilar-membrane responses to clicks: evidence for two modes of cochlear mechanical excitation. *J. Acoust. Soc. Am.* 124:1080–1092, 2008.
- LYON RF. Automatic gain control in cochlear mechanics. In: Dallos P, Geisler CD, Matthews JW, Ruggiero MA, Steele CR (eds) *The Mechanics and Biophysics of Hearing*. Berlin, Springer, pp. 395–402, 1990.
- LYON RF. All-pole models of auditory filtering. In: Lewis ER, Long GR, Lyon RF, Narins PM, Steele CR, Hecht-Poinar E (eds) *Diversity in Auditory Mechanics*. Singapore, World Scientific, pp. 205–211, 1997.
- MARMARELIS PZ, MARMARELIS VZ. *Analysis of Physiological Systems: The White Noise Approach*. New York, Plenum, 1978.
- MÖLLER AR. Frequency selectivity of single auditory-nerve fibers in response to broadband noise stimuli. *J. Acoust. Soc. Am.* 62:135–142, 1977.
- OXENHAM AJ, BACON SP. Cochlear compression: perceptual measures and implications for normal and impaired hearing. *Ear Hear.* 24:352–366, 2003.

- PAPOULIS A. *The Fourier Integral and its Applications*. New York, McGraw-Hill, 1962.
- PAPOULIS A. *Signal Analysis*. New York, McGraw-Hill, 1977.
- PAPOULIS A. *Probability, Random Variables and Stochastic Processes*. New York, McGraw-Hill, 1984.
- RECIO A, NARAYAN SS, RUGGERO MA. Wiener-kernel analysis of basilar-membrane responses to white noise. In: Lewis ER, Long GR, Lyon RF, Narins PM, Steele CR, Hecht-Poinar E (eds) *Diversity in Auditory Mechanics*. Singapore, World Scientific Publishing, pp. 325–331, 1997.
- RECIO A, RHODE WS. Basilar membrane responses to broadband stimuli. *J. Acoust. Soc. Am.* 108:2281–2298, 2000.
- RECIO A, RICH NC, NARAYAN SS, RUGGERO MA. Basilar-membrane responses to clicks at the base of the chinchilla cochlea. *J. Acoust. Soc. Am.* 103:1972–1989, 1998.
- RECIO-SPINOSO A, TEMCHIN AN, VAN DIJK P, FAN Y-H, RUGGERO MA. Wiener-kernel analysis of responses to noise of chinchilla auditory-nerve fibers. *J. Neurophysiol.* 93:3615–3634, 2005.
- RHODE WS. Basilar membrane mechanics in the 6–9 kHz region of sensitive chinchilla cochleae. *J. Acoust. Soc. Am.* 121:2792–2804, 2007.
- RHODE WS, RECIO A. Study of mechanical motions in the basal region of the chinchilla cochlea. *J. Acoust. Soc. Am.* 107:3317–3332, 2000.
- RICE SO. Mathematical analysis of random noise. In: Wax N (ed) *Selected Papers on Noise and Stochastic Processes*. New York, Dover, pp. 133–294, 1954.
- RINGACH D, SHAPLEY R. Reverse correlation in neurophysiology. *Cogn. Sci.* 28:147–166, 2004.
- ROBLES L, RUGGERO MA. Mechanics of the mammalian cochlea. *Physiol. Rev.* 81:1305–1352, 2001.
- RUGGERO MA, RICH NC, RECIO A, NARAYAN SS, ROBLES L. Basilar-membrane responses to tones at the base of the chinchilla cochlea. *J. Acoust. Soc. Am.* 101:2151–2163, 1997.
- SCHETZEN M. *The Volterra and Wiener Theories of Nonlinear Systems*. Malabar, FL, Krieger, 1989.
- SHERA CA. Intensity-invariance of fine time structure in basilar-membrane click responses: Implications for cochlear mechanics. *J. Acoust. Soc. Am.* 110:332–348, 2001.
- TAN Q, CARNEY LH. A phenomenological model for the responses of auditory-nerve fibers. II. Nonlinear tuning with a frequency glide. *J. Acoust. Soc. Am.* 114:2007–2020, 2003.
- TEMCHIN AN, RICH NC, RUGGERO MA. Threshold tuning curves of chinchilla auditory-nerve fibers. I. Dependence on characteristic frequency and relation to the magnitudes of cochlear vibrations. *J. Neurophysiol.* 100:2889–2898, 2008.
- TEMCHIN AN, RICH NC, RUGGERO MA. Threshold tuning curves of chinchilla auditory-nerve fibers predict cochlear phase-frequency curves and impulse-response frequency glides. *Assoc. Res. Otolaryngol. Mid-Wint. Meet. Abst.* 32:209, 2009.
- VAN DER HEIJDEN M. Cochlear gain control. *J. Acoust. Soc. Am.* 117:1223–1233, 2005.
- VOLTERRA V. *Theory of Functionals and of Integral and Integro-Differential Equations*. New York, Dover, 1959.
- WICKESBERG RE, DICKSON JW, GIBSON MM, GEISLER CD. Wiener kernel analysis of responses from anteroventral cochlear nucleus neurons. *Hear Res.* 14:155–174, 1984.
- ZWISLOCKI JJ, SZYMKO YM, HERTIG IX. The cochlea is an automatic gain control system after all. In: Lewis ER, Long GR, Lyon RF, Narins PM, Steele CR, Hecht-Poinar E (eds) *Diversity in Auditory Mechanics*. Singapore, World Scientific, pp. 354–360, 1997.